

Two Distinct Mechanisms of Inhibition of LpxA Acyltransferase Essential for Lipopolysaccharide Biosynthesis

Wooseok Han,¹ Xiaolei Ma,¹ Carl J. Balibar, Christopher M. Baxter Rath, Bret Benton, Alun Bermingham, Fergal Casey, Barbara Chie-Leon, Min-Kyu Cho, Andreas O. Frank, Alexandra Frommlet, Chi-Min Ho, Patrick S. Lee, Min Li, Andreas Lingel, Sylvia Ma, Hanne Merritt, Elizabeth Ornelas, Gianfranco De Pascale, Ramadevi Prathapam, Katherine R. Prosen, Dita Rasper, Alexey Ruzin, William S. Sawyer, Jacob Shaul, Xiaoyu Shen, Steven Shia, Micah Steffek, Sharadha Subramanian, Jason Vo, Feng Wang, Charles Wartchow, and Tsuyoshi Uehara*

Cite This: <https://dx.doi.org/10.1021/jacs.9b13530>

Read Online

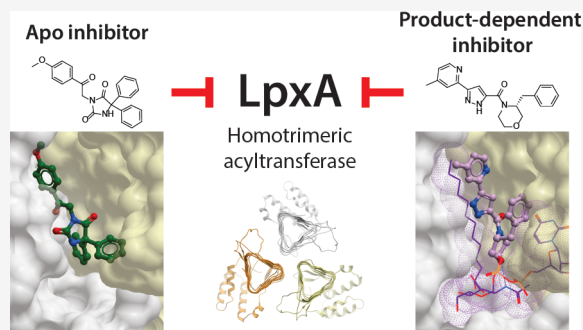
ACCESS |

Metrics & More

Article Recommendations

Supporting Information

ABSTRACT: The lipopolysaccharide biosynthesis pathway is considered an attractive drug target against the rising threat of multi-drug-resistant Gram-negative bacteria. Here, we report two novel small-molecule inhibitors (compounds 1 and 2) of the acyltransferase LpxA, the first enzyme in the lipopolysaccharide biosynthesis pathway. We show genetically that the antibacterial activities of the compounds against efflux-deficient *Escherichia coli* are mediated by LpxA inhibition. Consistently, the compounds inhibited the LpxA enzymatic reaction in vitro. Intriguingly, using biochemical, biophysical, and structural characterization, we reveal two distinct mechanisms of LpxA inhibition; compound 1 is a substrate-competitive inhibitor targeting apo LpxA, and compound 2 is an uncompetitive inhibitor targeting the LpxA/product complex. Compound 2 exhibited more favorable biological and physicochemical properties than compound 1 and was optimized using structural information to achieve improved antibacterial activity against wild-type *E. coli*. These results show that LpxA is a promising antibacterial target and imply the advantages of targeting enzyme/product complexes in drug discovery.



1. INTRODUCTION

Bacterial antibiotic resistance is a growing crisis worldwide. In particular, untreatable and hard-to-treat infections by multi-drug-resistant Gram-negative bacteria are a serious issue as they are becoming prevalent among patients in medical facilities.^{1,2} Multidrug resistance mechanisms in Gram-negative pathogens consist mainly of antibiotic-modifying enzymes, active efflux, loss of outer membrane porins, target mutations, as well as combinations of these factors.³ Depending on their structure–activity relationships, novel antibacterial agents directed at new cellular targets could address such mechanisms of clinical resistance. However, target-based biochemical assays have only rarely provided leads with potent antibacterial activity against wild-type Gram-negative bacteria.^{4,5} This is because efflux and permeability barriers make many intracellular targets inaccessible to small-molecule enzyme inhibitors. One strategy to address the limitation is to directly inhibit the lipopolysaccharide (LPS) biogenesis and transport pathways which enable these barriers.^{6–16}

LPS, also known as endotoxin, is composed of a lipid A anchor that forms the outer leaflet of the outer membrane, a core oligosaccharide, and covalently linked repeating poly-

saccharide O-antigen that extends out from the cell surface.¹⁷ Lipid A is produced by enzymes localized in the cytoplasm or the inner leaflet of the cytoplasmic membrane.¹⁷ Since lipid A is essential for growth and structural integrity of most Gram-negative bacteria, small-molecule inhibitors of lipid A biosynthesis prevent growth or restore the activity of antibiotics with intracellular targets that could not otherwise be reached.^{14,15,18} Furthermore, inhibition of lipid A biosynthesis can reduce the levels of endotoxin that are released during antibiotic treatment.¹⁹ Therefore, lipid A biosynthesis has been viewed as a promising target for the discovery of new antibacterials. The most advanced programs targeting lipid A are inhibition of LpxC, the second enzyme of the pathway.¹⁴ An LpxC inhibitor reached clinical trials; however, development was halted due to toxicity.¹² Inhibition of other enzymes in the lipid A

Received: December 16, 2019

biosynthesis pathway is also appealing, but only a few small-molecule inhibitors have been reported.^{16,20}

LpxA UDP-*N*-acetylglucosamine acyltransferase is the first enzyme in the lipid A biosynthesis pathway.¹⁷ This enzyme is conserved and essential in difficult-to-treat Gram-negative pathogens, with the exception of *Acinetobacter baumannii* which can grow without LPS under laboratory growth conditions.^{21,22} In *Escherichia coli*, LpxA catalyzes the transfer of *R*-3-hydroxymyristate from acyl carrier protein (ACP) to the 3-hydroxyl group of UDP-*N*-acetylglucosamine (UDP-GlcNAc), generating UDP-3-*O*-(3-OH-acyl)-GlcNAc (Figure 1a).¹⁷ Remarkably, the reaction catalyzed by *E. coli* LpxA is

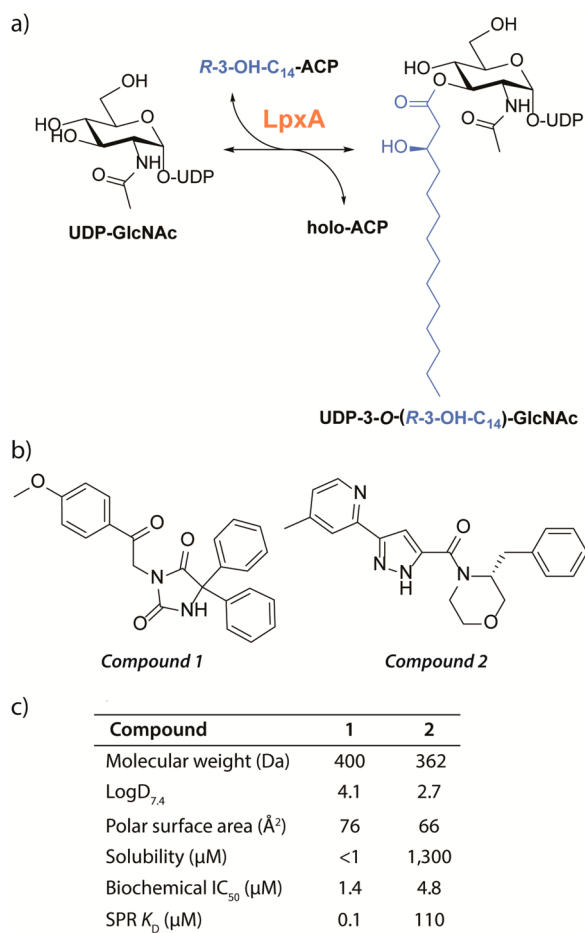


Figure 1. *E. coli* LpxA reaction and the chemical structures and properties and biological activities of compounds 1 and 2. (a) *E. coli* LpxA reaction. LpxA utilizes *R*-3-hydroxymyristoyl-acyl-carrier-protein (*R*-3-OH-C₁₄-ACP) to transfer the fatty acyl chain to UDP-GlcNAc, generating UDP-3-*O*-(*R*-3-OH-C₁₄)-GlcNAc. (b) Chemical structures of compounds 1 and 2. (c) Physicochemical properties and in vitro activities of the compounds.

reversible with an unfavorable equilibrium constant ($K_{eq} \approx 0.01$).^{23,24} LpxA contains an unusual, left-handed parallel β -helix fold and forms a soluble stable homotrimer constituting three active site pockets at the subunit interfaces.^{25–27} Crystal structures of *E. coli* LpxA in complex with its substrate UDP-GlcNAc,²⁸ product UDP-3-*O*-(*R*-3-hydroxymyristoyl)-GlcNAc,²⁸ and peptide inhibitors^{29–33} have been previously described, providing important insights into the catalytic mechanism and target validation. One of the peptide inhibitors was used as a tool molecule for development of assays to screen

for compounds that bind LpxA.³⁴ However, these peptide inhibitors cannot be chemical starting points for development of antibacterial agents targeting cytoplasmic LpxA due to the lack of the delivery system. Although small-molecule inhibitors against *Pseudomonas aeruginosa* LpxA and LpxD were reported recently,¹⁶ no LpxA inhibitor having antibacterial activity has been publicly disclosed.

Here, we present the small-molecule inhibitors of *E. coli* LpxA, compounds 1 and 2 (Figure 1b). The compounds are among the hits from cell-based screenings of Novartis compound collections for bacterial growth inhibitors and show antibacterial activity against efflux-deficient *E. coli* ($\Delta tolC$) with no measurable eukaryotic cell cytotoxicity or hemolysis at 100 μ M. Genetic target identification and in vitro inhibitory activity in the LpxA-specific biochemical assay indicated that both compounds were LpxA inhibitors with antibacterial activity mediated by the target inhibition. Intriguingly, we found that the compounds showed distinct mechanisms of inhibition. Using biochemical and biophysical characterizations and X-ray crystallography, we demonstrate that compound 1 is an inhibitor of apo LpxA and that compound 2 inhibits LpxA only in the presence of the product UDP-3-*O*-(*R*-3-hydroxymyristoyl)-GlcNAc. Compound 2 was prioritized for follow up and optimized to achieve a minimal inhibitory concentration (MIC) of 16 μ g/mL against wild-type *E. coli*. Our findings establish that the LpxA/product complex is a promising target for antibiotic discovery and provide advantages to design product-dependent inhibitors for target-based drug discovery.

2. RESULTS

2.1. Compound 1 Is an Apo LpxA Inhibitor. To identify the cellular target of the antibacterial active compound 1, we performed mutant selection of *E. coli* $\Delta tolC$ cells and yielded a mutant that had a FabZ A146D substitution. Mutations in *fabZ* are known to suppress the growth defect of *lpxA* and *lpxC* mutants and also reduce the activity of LpxC inhibitors^{35–37} and an LpxD inhibitor.²⁰ Therefore, we postulated that compound 1 inhibited one or more of the Lpx enzymes rather than FabZ. Consistent with this, three *fabZ* mutants that encoded different FabZ substitutions were less susceptible to compound 1 and the LpxC inhibitor CHIR-090 (Table 1). We then examined whether overexpression of a selection of essential lipid A biosynthetic enzymes altered susceptibility to compound 1. Susceptibility was reduced only by LpxA overexpression (Table 1), suggesting that the antibacterial activity of compound 1 was mediated by inhibition of LpxA. To show whether the compound directly inhibited LpxA, we tested compound 1 in an in vitro biochemical assay using a solid-phase-extraction mass-spectrometry (SPE-MS)-based read out for the LpxA product. Compound 1 showed a half-maximal inhibitory concentration (IC₅₀) of 1.4 μ M, indicating that compound 1 is an LpxA inhibitor (Figure 1c).

To determine the mechanism of inhibition of compound 1, we tested the compound in a surface plasmon resonance (SPR) binding assay to measure binding affinity for apo LpxA. We found that compound 1 bound surface-immobilized LpxA with a K_D of 0.1 μ M (Figure 2a), suggesting that this compound inhibits LpxA by binding the apo form. Enzymatic characterization was also performed using titration of each of the two LpxA substrates (3-OH-acyl-ACP and UDP-GlcNAc). Compound 1 showed inhibition competitive with 3-OH-acyl-ACP and noncompetitive to UDP-GlcNAc (Figure 3), which is

Table 1. MICs of the LpxA Inhibitors and the LpxC Inhibitor CHIR-090^a

strain	description	compound 1		compound 2		CHIR-090	
		MIC	fold shift	MIC	fold shift	MIC	fold shift
ATCC 25922	<i>E. coli</i> clinical isolate	>16		>128		ND ^b	
MG1655	<i>E. coli</i> K-12	>16		>128		ND	
VECO2526	<i>E. coli</i> $\Delta tolC$	0.5	1	2	1	0.015	1
TUP0115*	$\Delta tolC$ pLacZ α ↑	0.5	1	2	1	0.008	0.5
TUP0116*	$\Delta tolC$ pLpxA↑	>16	>32	>64	>32	0.06	4
TUP0118*	$\Delta tolC$ pLpxC↑	0.5	1	2	1	0.125	8
TUP0119*	$\Delta tolC$ pLpxD↑	0.5	1	2	1	0.015	1
ARA0016	$\Delta tolC$ FabZ _{A78V}	>16	>32	1	0.5	0.25	16
TUP0074	$\Delta tolC$ FabZ _{P56L}	>16	>32	2	1	0.25	16
TUP0042	$\Delta tolC$ FabZ _{C145Y}	>16	>32	2	1	0.25	16
CDY0154	<i>E. coli</i> $\Delta 9$ efflux	0.5	1	2	1	0.075	1
TUP0093	$\Delta 9$ efflux LpxA _{Q73L}	1	2	64	32	0.075	1
TUP0092	$\Delta 9$ efflux AccB _{E128K}	0.5	1	32	16	0.075	1
TUP0097	$\Delta 9$ efflux InfA _{R66H}	1	2	32	16	0.075	1

^aThe values are modes of MIC values measured in at least two independent experiments. MICs for the strains with asterisks were determined in the presence of 100 μ M IPTG to induce the gene expression (up-arrow). TUP0115 carries a control vector expressing LacZ α . The unit of MIC values is μ g/mL. The MIC fold shifts with ≥ 4 are shown in bold. Although compound 1 was tested at the maximum concentration of 128 μ g/mL in the MIC assay, precipitation was observed at 32, 64, and 128 μ g/mL. Due to the precipitation, >16 μ g/mL is reported when no inhibition of growth was observed at 16 μ g/mL and higher concentrations. ^bND: not determined.

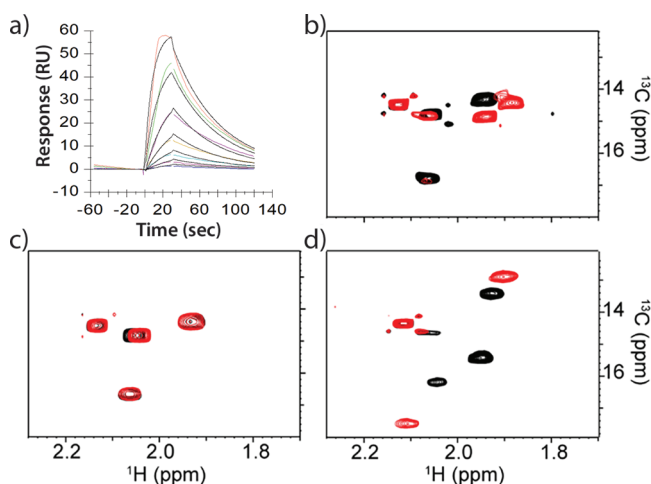


Figure 2. Biophysical characterization of compounds 1 and 2. (a) SPR sensorgram. Avi-tagged LpxA was immobilized to the SPR chip surface. The responsive units for compound 1 (6 point concentrations, 2 \times dilutions, top 100 μ M) plotted are shown over time. The kinetic K_D of compound 1 determined with a 1:1 binding was 0.1 μ M. SPR sensorgram for compound 2 is shown in Figure S3. (b–d) Protein-observed 2D ¹H–¹³C HMQC (heteronuclear multiple quantum coherence) spectra of the labeled amino acid residues (MILVAT) of LpxA. Shown are the peaks representing the methyl group of the LpxA methionine side chain in the absence (black) or presence (red) of compound 1 (b) or compound 2 (c). LpxA peaks with the product UDP-3-*O*-(*R*-3-hydroxymyristoyl)-GlcNAc are shown in the absence (black) or presence (red) of compound 2 (d). Peak shifts represent ligand binding to LpxA. The concentrations in samples were 80 μ M isotope-labeled LpxA, 100 μ M compound, and 150 μ M LpxA product. The entire methyl regions of the spectra are shown in Figure S4.

consistent with apo LpxA being its target. We further obtained the LpxA X-ray costructure with compound 1 at 2.1 Å by soaking (Figure 4a, Figure S5). Compound 1 clearly bound to apo LpxA (three inhibitors per trimer) by occupying a large portion of the acyl chain binding pocket. The hydantoin motif of compound 1 engaged two adjacent LpxA subunits by H-bonding interactions to Q161 of one subunit and G155 of the

other subunit. The binding site for the compound also included a smaller hydrophobic pocket lined by M118, I134, A136, and I152. Interestingly, G155 has previously been implicated in pantetheine binding to *Leptospira interrogans* LpxA.³⁸ Collectively, these results reveal that compound 1 inhibits LpxA function by directly targeting the apo enzyme.

2.2. Compound 2 Also Targets LpxA in *E. coli*. To identify the cellular target of compound 2, we utilized a gene overexpression library in the *E. coli* strain lacking nine efflux pumps (CDY0154). The library was constructed using the mobile plasmid collection³⁹ where every *E. coli* gene is expressed from an inducible promoter of a low copy plasmid. Selection by compound 2 yielded only the *lpxA* clone in 40 separately isolated colonies, suggesting that compound 2 was also an LpxA inhibitor. This was further confirmed with reduced susceptibility by overproduction of LpxA expressed from a different plasmid backbone, but not by LpxC or LpxD (Table 1). We then tested the impact of *fabZ* mutations on compound susceptibility. Unexpectedly, the *fabZ* mutant strains were equally susceptible to compound 2 in contrast to their reduced susceptibility to compound 1 and the LpxC inhibitor CHIR-090 (Table 1).

To further understand the cellular target of compound 2, we isolated mutants with reduced susceptibility by passaging CDY0154 cells in the presence of compound 14, an analogue of compound 2 (Figure S2). Colonies arose at a frequency of approximately 10⁻⁸ on agar containing compound 14 at 16 or 32 μ g/mL. Among a total of 18 colonies isolated by mutant selection, three mutants were used for genome sequencing and susceptibility tests. Mutant TUP0093 had an LpxA Q73L substitution and was 32-fold less susceptible to compound 2 (Table 1). The other two mutants were 16-fold less susceptible and had mutations in *accB* or *infA* (Table 1). InfA is an initiation factor for translation,⁴⁰ and AccB is a component of the acetyl-CoA carboxylase (Acc) complex that catalyzes the first reaction of fatty acid biosynthesis.⁴¹ Neither the *accB* nor the *infA* mutation affected the MICs of compound 1 or CHIR-090 (Table 1), which together with the susceptibility of the *fabZ* mutants suggested a specific mechanism to reduce

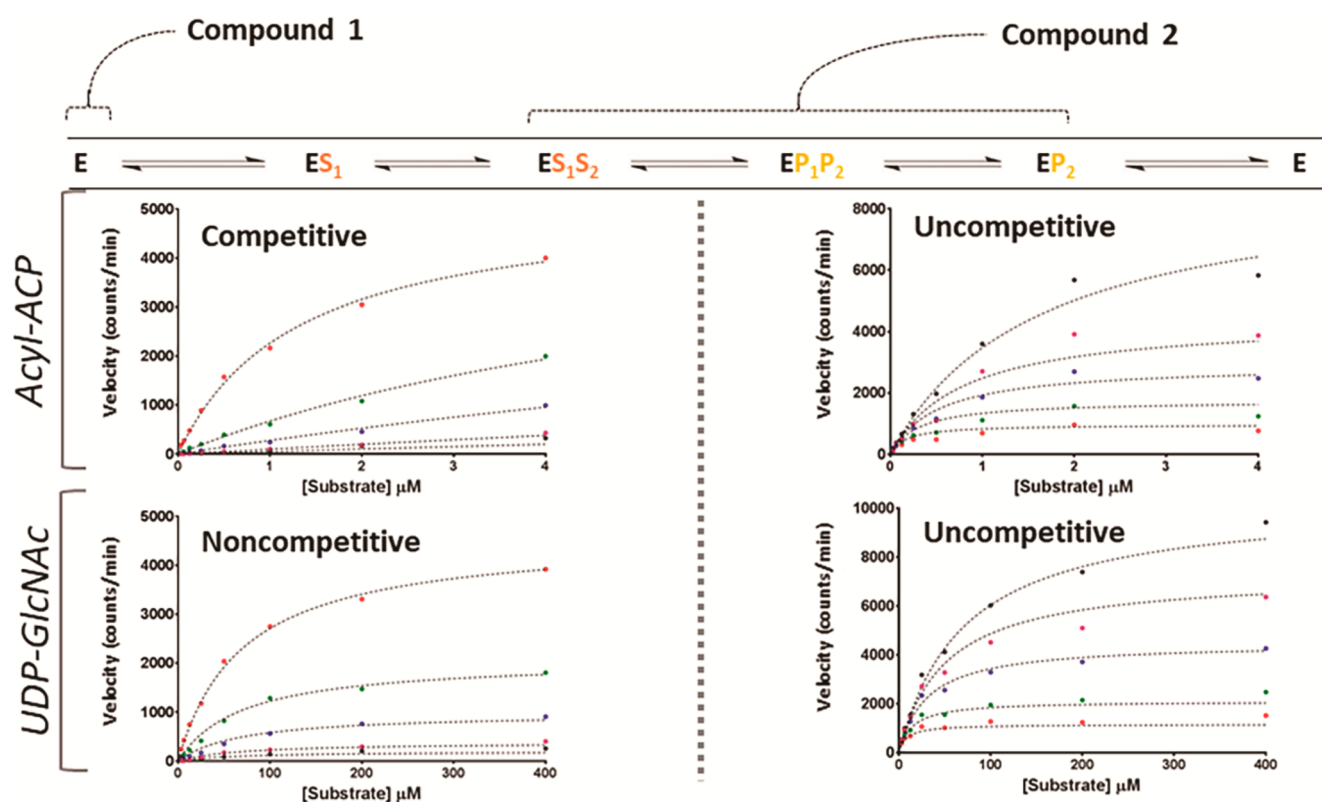


Figure 3. Biochemical characterization of compounds 1 and 2. The scheme of the enzymatic steps in the LpxA reaction is shown on the top. (left) Compound 1 showed competitive inhibition to 3-OH-acyl-ACP and noncompetitive to UDP-GlcNAc. (right) Compound 2 showed uncompetitive inhibition to both substrates. The inhibitor concentrations used were 0, 0.48, 1.45, 4.35, and 8.7 μM for compound 1, and 0, 1.3, 4.1, 12.3, and 25 μM for compound 2. Data are mean of two assays. The signals (counts) of the product were measured using SPE-MS.

susceptibility to compound 2. Since *accB* and *infA* are also essential for growth,⁴² we cannot exclude the possibility that compound 2 inhibits one or both protein functions. However, compound 2 showed direct inhibition of the *in vitro* LpxA reaction with an IC_{50} of 4.8 μM (Figure 1c), indicating that compound 2 is an LpxA inhibitor. The distinct resistant profiles suggest that the two inhibitors, compounds 1 and 2, differed in their mode of LpxA inhibition.

2.3. Compound 2 Is a Product-Dependent LpxA Inhibitor. Despite the biochemical IC_{50} of 4.8 μM , compound 2 bound weakly to apo LpxA ($\text{SPR } K_D = 110 \mu\text{M}$, Figure 1c, Figure S3). This discrepancy between the biophysical and biochemical potency of compound 2 prompted us to further investigate its underlying mechanism of action. Enzyme kinetics studies showed that compound 2 was uncompetitive with both LpxA substrates (Figure 3), consistent with the weak binding to apo LpxA. This result also indicated dependence on the presence of either a substrate or a product for inhibition by compound 2. Based on the unfavorable forward reaction of LpxA²³ and the stable enzyme/product complex demonstrated by the crystal structure with UDP-3-O-(R-3-hydroxymyristoyl)-GlcNAc,²⁸ we postulated that compound 2 might bind the LpxA/product complex. To examine the binding mechanism, we developed a two-dimensional protein-observed HMQC NMR assay^{43,44} for *E. coli* LpxA, using selective incorporation of ¹H, ¹³C isotope labels at all methyl positions of CH₃-containing amino acids (Met, Ile, Leu, Val, Ala, and Thr, but not Ile C γ). As expected, robust chemical shift perturbations (CSPs) were observed when isotope-labeled LpxA was incubated with compound 1 (Figure 2b). In contrast, few small CSPs of

LpxA resonances were observed upon addition of 100 μM of compound 2, consistent with weak binding to apo LpxA (Figure 2c). As we hypothesized, drastic CSPs and signal broadening were observed for product-bound LpxA in the presence of compound 2 (Figure 2d, Figure S4). These results indicate that compound 2 inhibits the LpxA reaction in a product-dependent manner.

2.4. LpxA Crystal Structure in Complex with Product UDP-3-O-(R-3-hydroxymyristoyl)-GlcNAc and Compound 2. To further validate and characterize the LpxA/product complex as the molecular target of compound 2, unliganded LpxA crystals were soaked with 2 mM compound 2 and 40 mM UDP-3-O-(R-3-hydroxymyristoyl)-GlcNAc. The crystals diffracted to 1.8 Å resolution with excellent geometry as assessed with Mol-ProBity⁴⁵ (Table S3). Compared to the LpxA structure in complex with its product,²⁸ additional electron density that fitted compound 2 was clearly observed and belonged to the R-enantiomer (Figure S5), representing the biologically active form of compound 2. Compound 2 occupied the pantetheine site and formed extensive interactions with both the LpxA protein and LpxA product UDP-3-O-(3-OH-acyl)-GlcNAc (Figure 4b). In the ternary complex, the product followed the “down” conformation observed in the LpxA/UDP-3-O-(R-3-hydroxydecanoyl)-GlcNAc complex²⁸ more closely than the “up” conformation observed in the LpxA/UDP-3-O-(R-3-hydroxymyristoyl)-GlcNAc complex²⁸ (Figure S6). Intriguingly, five of six heteroatoms of compound 2 were involved in direct or water-mediated H-bonds. Specifically, the pyridine and pyrazole moieties formed direct H-bonds with the backbone carbonyl of G173 and H160 of

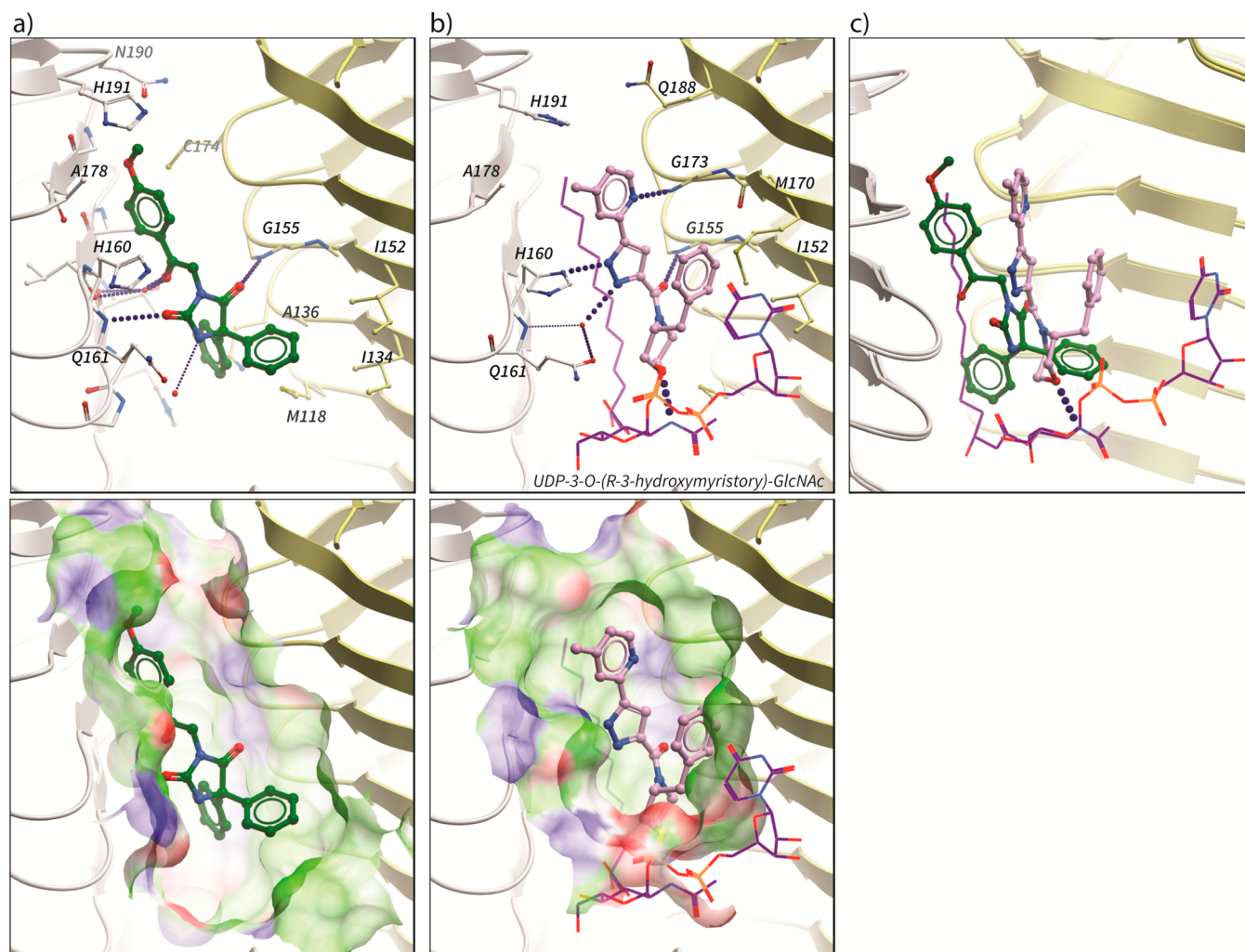


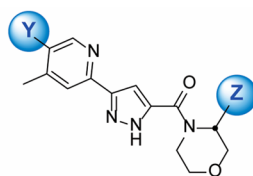
Figure 4. Co-structures of LpxA in complex with compound 1 and 2. The X-ray crystal structures in complex with compound 1 (a) and in complex with the product and compound 2 (b), and an overlay of compound 1 and 2/LpxA product (c) are shown. The asymmetric unit contains one LpxA monomer in complex with one LpxA product (UDP-3-O-(R-3-hydroxymyristoyl)-GlcNAc) and one compound, and the biologically functional trimer lies on the crystallographic 3-fold axis. LpxA is shown as a cartoon ball and sticks representation with carbon colored white for subunit 1 and yellow for subunit 2, oxygen colored red, and nitrogen colored blue. Compounds are shown as ball and sticks with carbon colored green (compound 1) and purple (compound 2). LpxA product (b, c) is shown as sticks with carbon colored purple. (bottom) The binding pockets for the compounds 1 (a) and 2 (b) are shown with the representation of hydrophobic (green), positive-charged (red), and negative-charged (blue) surface.

LpxA, respectively. The pyrazole formed a water-mediated interaction with Q161. The morpholine moiety was directly associated with the nitrogen atom at the C2 position of the GlcNAc moiety of the product. The benzyl group mediated hydrophobic interactions with LpxA M170 and I152. This structure reveals why compound 2 shows a low affinity for apo LpxA in SPR and NMR and is consistent with product-dependent inhibition.

2.5. Structure-Based Compound Design Improved the Antibacterial Activity. Although the LpxA inhibitor compounds 1 and 2 exhibited good activity against the efflux-deficient *E. coli* strains, both did not inhibit growth of the *E. coli* ATCC 25922 clinical isolate even at 128 $\mu\text{g}/\text{mL}$ (Table 1). To improve cellular activity against wild-type *E. coli*, we initiated structure-based optimization of compound 2 with favorable properties for Gram-negative antibacterial agents that must pass through bacterial outer and inner membranes to reach their targets;⁴⁶ that is, compound 2 had higher solubility, lower log *D* (pH 7.4), and lower molecular weight than compound 1 (Figure 1c). Furthermore, the binding pocket of the LpxA/

product complex was much smaller and more polar than that of the apo enzyme (Figure 4). These attributes made compound 2 the more progressible chemical starting point for optimization for potency against wild-type *E. coli*.

We designed and synthesized analogues of compound 2 using structural information and in consideration of the physicochemical properties preferred for antibiotics that are active against Gram-negative bacteria.^{46,47} In the X-ray cocrystal structure of compound 2 and the LpxA/product complex, the electron density of the benzyl moiety was weaker than that of the other parts of the molecule. This indicated that the benzyl group was partly flexible. Therefore, we expected that optimization in this region could increase the inhibitory potency while maintaining or improving physicochemical properties. Removal or replacement of the benzyl with alkyl groups and heterocyclic rings, such as pyridines and pyrazoles (compounds 3–5) resulted in a significant loss of potency in biochemical and MIC assays (Figure 5), suggesting that the benzyl moiety is important for maintaining the antibacterial effect. With respect to substitutions to the benzyl ring, ortho-



Cpd #	Y	Z	MW	logD _{7.4}	PSA	Sol (pH 7.4) (mM)	LpxA IC ₅₀ (μM)	MIC (μg/mL)					
								Ec WT	Ec ΔtolC	Ec Δ9pump	Ec Δ9pump LpxA _{O73L}	Ec imp4213	Ec ΔacrB
2	H		362	2.7	66	1.3	4.8	>128	2	1	32	4	4
3	H	H	272	1	71	N/A	>250	>128	>128	>128	>128	>128	N/A
4	H		314	2	71	>1.6	148	>128	64	16	>128	64	N/A
5	H		363	1.6	84	>1.1	86	>128	32	16	>128	64	N/A
6	H		380	2.7	71	0.18	3	>128	0.5	0.5	8	4	1
7	H		397	3	71	1.08	2.9	>128	0.25	0.25	4	4	N/A
8	H		393	2.3	80	1.7	11	>128	1	0.5	16	4	N/A
9	H		410	2.5	80	1.3	2.5	64	0.25	0.125	4	1	N/A
10	H		410	N/A	80	1.2	28	>128	8	4	64	32	N/A
11	H		427	3.1	80	0.62	0.5	32	<0.125	<0.125	2	2	0.25
12	H		362	N/A	71	N/A	171	>128	>128	>128	>128	>128	N/A
13	NH ₂		442	2.3	106	1.03	0.6	16	<0.125	<0.125	2	1	N/A

Figure 5. Physicochemical properties and biological activities of analogues of compound 2. Compound 10 (compound 9 enantiomer) was 94% pure after chiral separation. As it contained a small amount of compound 9, it showed weak biological activities. Compound 12 (compound 2 enantiomer) and compound 13 were >99% and 90% pure, respectively. MW, molecular weight; PSA, polar surface area; Sol, solubility; Ec, *E. coli*; Ec WT, ATCC 25922; Ec ΔtolC, JW5503-1; Ec ΔacrB, JW0451; N/A, not applicable.

substituents favorably influenced antibacterial activity in comparison with meta- or para-substituents. In particular, the addition of a fluoro group at the ortho-position of the benzyl group (compound 6) led to 4-fold improvement in MIC against the efflux-deficient *E. coli* ΔtolC. Likewise, compound 7 having ortho-chloro substituent and compound 8 having ortho-methoxy substituent increased an antibacterial effect on *E. coli* ΔtolC. To evaluate the effect of the ortho-substitution on compound binding, we obtained LpxA cocrystal structures with compounds 6 and 8 in the presence of UDP-3-O-(R-3-hydroxymyristoyl)-GlcNAc. The structures showed that the ortho-substituents in compounds 6 and 8 were located in different regions: the fluoro group in compound 6 faced toward the protein, and the methoxy group in compound 8 was exposed to solvents (Figure 6a, Figure S5). In both cases, the benzyl ring was shifted toward the protein by pulling or pushing the ring, respectively. In addition, the ortho-substituted benzyl groups were much better defined in the electron density map compared to the benzyl group of compound 2 (Figure S5). Based on this structural information, we prepared compounds 9

and 11 (Figure 5) that had substituents at the two different ortho-positions. Compound 11 having chloro and methoxy substituents at the ortho-positions showed better biochemical IC₅₀ than compound 9 having fluoro and methoxy substituents, suggesting a better ortho-substitution of chloro than fluoro for ligand binding. Compound 11 exhibited slightly better antibacterial activity against a wild-type clinical isolate, *E. coli* ATCC 25922 (MIC = 32 μg/mL), than compound 9. Furthermore, a polar functional group at the ortho position of the methyl in the pyridine ring was anticipated to make a hydrogen bond interaction with Q188. Compound 13 having an amino group in the pyridine ring showed an MIC of 16 μg/mL against wild-type *E. coli*. Using the X-ray crystallography, we confirmed a hydrogen bond interaction of the amino group of compound 13 made with Q188 of one subunit of LpxA and found additional interaction with His191 of the other subunit (Figure 6b). The antibacterial activities of these analogues were very likely to be mediated by LpxA inhibition because of the reduction of cell susceptibility by the LpxA Q73L variant (Figure 5) and the lower activities shown by the enantiomers of

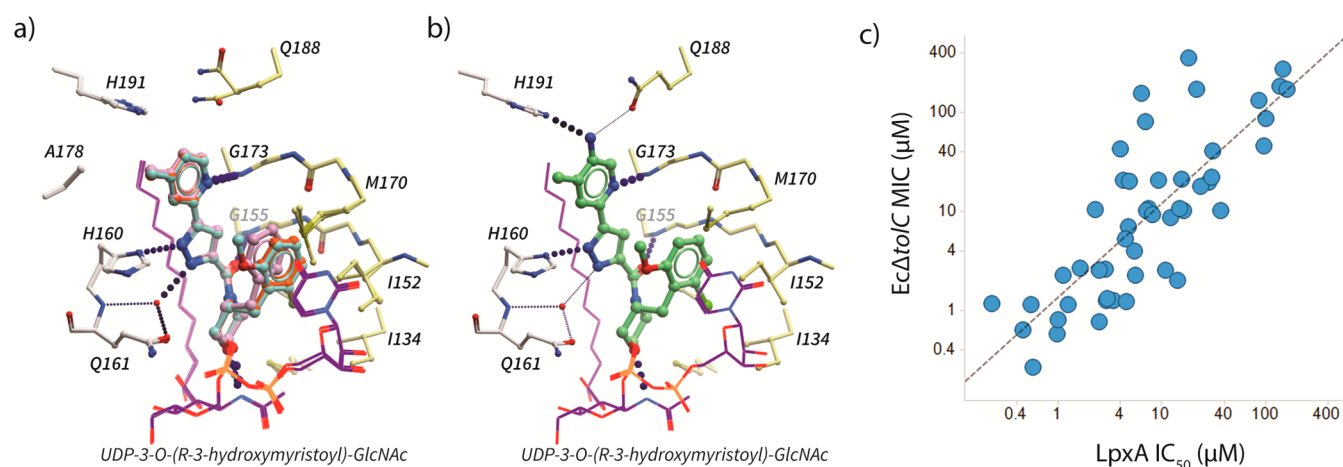


Figure 6. Structure-guided optimization of compound 2. (a) An overlay of the LpxA crystal structures in complex with compounds 2 (purple), 6 (red), and 8 (aqua) and with the product. The ortho fluoro group (compound 6) and the ortho methoxy group (compound 8) were observed in opposite orientations in the structures. (b) X-ray crystal structures in complex with the product and compound 13. (c) Correlation of in vitro enzyme inhibition (LpxA IC₅₀) and MIC against *E. coli* ΔtolC for LpxA inhibitors ($n = 49$, blue circle). Compounds that showed $>250 \mu\text{M}$ IC₅₀ or $>128 \mu\text{g}/\text{mL}$ EcΔtolC MIC were not plotted. A simple linear regression is shown as a dashed line ($R^2 = 0.635$).

compound 2 and 9 (compound 12 and 10, respectively). Consistently, we found a moderate linear correlation between the biochemical inhibition and the antibacterial activity against *E. coli* ΔtolC for analogues of compound 2 (Figure 6c). Taken together, the introduction of three different functional groups (chloro, methoxy, and amino groups) resulted in an 8-fold improvement in both biochemical inhibition and antibacterial activity, leading to an MIC of 16 μg/mL against wild-type *E. coli*.

3. DISCUSSION

Here, we report novel LpxA small-molecule inhibitors. Notably, the inhibitors had two distinct mechanisms of action: the substrate-competitive inhibitor compound 1 and the product-dependent inhibitor compound 2. While substrate-competitive inhibitors are commonly identified in target-based screenings, product-dependent inhibitors are more unusual. An example is triclosan, the antibiotic that inhibits FabI only in the presence of the product NAD⁺ and forms a tight ternary complex.⁴⁸ Overall, the product-dependent inhibitor compound 2 showed more favorable biological and chemical properties than compound 1.

Resistance profiling was one way to distinguish between the two LpxA inhibition mechanisms. Mutations in *fabZ* decreased susceptibility to compound 1 as well as to inhibitors of LpxC and LpxD. This is probably because altered FabZ proteins are less active, resulting in an increased cellular level of R-3-hydroxymyristoyl-ACP which competes with compound 1 for binding to LpxA. This is analogous to the previously proposed mechanism of resistance by *fabZ* mutations to the substrate-competitive LpxC inhibitor CHIR-090.³⁵ In contrast, *fabZ* mutations did not affect the potency of compound 2, supporting its substrate-uncompetitive mechanism. Therefore, the increased metabolic flux to LPS biosynthesis that occurs in *fabZ* mutants should increase the IC₅₀ of substrate-competitive inhibitors of LpxA, LpxC, and LpxD but not influence the activity of the substrate-uncompetitive product-dependent inhibition of LpxA. LpxC inhibitors are in development for treatment of Gram-negative pathogens,^{8,14,49} and if an LpxC inhibitor is approved and used in the clinic, pathogens would be expected to acquire *fabZ* mutations over time. These mutants

would become cross-resistant to an apo LpxA inhibitor, but still susceptible to a product-dependent LpxA inhibitor.

The *lpxA* missense mutation that reduced compound 2 activity caused the substitution of Gln73 to Leu. The side chain of Q73 is located in the active site pocket and forms a direct hydrogen bond with the 3'-hydroxyl group of the product.²⁸ It was therefore unexpected that Q73 was not essential for LpxA activity and bacterial viability. There was no direct interaction between Q73 and compound 2 in the ternary complex structure, suggesting that Q73L may affect the configuration of product binding to LpxA, thereby reducing the affinity of compound 2 to the LpxA/product complex. The LpxA Q73L variant did not affect compound 1 activity, consistent with no direct interaction being present between compound 1 and Q73 in the LpxA/compound 1 costructure. The difference in susceptibility profiles for the two LpxA inhibitors makes the LpxA_{Q73L} mutant a useful tool for validating cellular on-target activity of chemical modifications around the compound 2 scaffold.

Using a structure-based inhibitor design, we could improve the antibacterial and biochemical activities of compound 2 by 8-fold. The most potent compound (compound 13) in the series showed sub-micromolar IC₅₀ and an MIC of 16 μg/mL against *E. coli* ATCC 25933, a clinical isolate. It is possible that the affinity for LpxA in the product-dependent inhibition mode is saturated or that it is limited by the affinity of the LpxA product. Product-dependent inhibition of FabI by triclosan is very potent (IC₅₀ in the nanomolar range), while the affinity of NAD⁺ for FabI is in the low millimolar range.^{48,50} In the case of triclosan, therefore, the potency of product-dependent inhibition does not depend on product affinity. It remains unclear whether the affinity of compound 2 is dependent on product affinity to LpxA. In the LpxA ternary complex, compound 2 interacted with both the product and residues in the LpxA active site. Thus, further optimization of product-dependent inhibitors for binding to LpxA protein residues is expected to lead to significant increases in affinity. In addition to affinity enhancement, compound 2 series needs further improvement in the MICs against clinical isolates of *E. coli* (and other Gram-negative pathogens) in order to move the LpxA

inhibitor forward on lead optimization. In general, understanding the chemical properties that facilitate compound accumulation in Gram-negative bacterial cells by overcoming outer membrane permeability and efflux is important for antibacterial discovery.^{4,51–53} However, universal guidelines that can be used to optimize compounds for better bacterial cell accumulation are not yet established because molecular descriptors for compound accumulation vary for each chemical scaffold.⁵³ Understanding of cell entry for this chemical series as well as insights into increasing binding affinity to the LpxA/product complex are necessary to further increase potency and accumulation in *E. coli*.

LpxA is structurally similar to LpxD, the acyltransferase that catalyzes the third step of lipid A biosynthesis, and shares the same substrate *R*-3-OH-acyl-ACP with LpxD. A peptide and a small molecule that inhibit or bind both LpxA and LpxD have been identified,^{16,30} supporting the possibility of a dual-targeting inhibitor of the two enzymes in the same pathway. The genetic data presented here indicate that both compound 1 and compound 2 specifically target LpxA in *E. coli*, which is consistent with the lack of significant inhibition of LpxD enzymatic activity detected for both compounds (data not shown). Other than *E. coli*, analogues of compound 2 exhibited MICs of 64 $\mu\text{g/mL}$ or higher against clinical isolates of Enterobacteriales including *Klebsiella pneumoniae* and *Enterobacter cloacae*. Since the amino acid sequence of LpxA is well conserved in Enterobacteriales, the compounds would likely target LpxA, but they did not prevent growth presumably because efflux and/or permeability barriers limited compound accumulation in the cytoplasm in these clinical isolates.

In *Pseudomonas aeruginosa*, neither compound 1 nor compound 2 (nor the analogues) was active even against drug-sensitized strains at 128 $\mu\text{g/mL}$. This is probably due to active site differences in *P. aeruginosa* LpxA that would interfere with inhibitor binding (Figure S7). While *E. coli* LpxA prefers *R*-3-hydroxymyristoyl-ACP as a substrate over the shorter fatty acyl variant *R*-3-hydroxydecanoyl-ACP, *P. aeruginosa* LpxA prefers the opposite.⁵⁴ In *P. aeruginosa* LpxA, Met169 serves to constrain the length of the acyl chain.^{27,54} With the preference for the shorter fatty acyl substrate, the active site pocket of *P. aeruginosa* LpxA is substantially smaller than that of *E. coli* LpxA. *P. aeruginosa* LpxA residue Met169 corresponds to *E. coli* LpxA residue Gly173, which forms a key hydrogen bond interaction to the pyridine of compound 2. Thus, it is expected that the scaffolds of *P. aeruginosa* LpxA inhibitors will be different from those identified here.

In conclusion, the identification of the inhibitors with the two distinct mechanisms of action and the improvement of the potency of the product-dependent inhibitor exhibit that LpxA is a promising antibacterial target against multi-drug-resistant Gram-negative bacteria. This work also suggests that LpxA overexpression is a useful method to identify compounds that target LpxA with various mechanisms of action in the cellular context. This genetic method is based on antibacterial activity of compounds and cannot be applied to identify inhibitors that are inactive or weakly active against efflux-deficient *E. coli*, nor those unaffected by LpxA overexpression (these compounds could potentially be identified by biochemical or biophysical assays). A distinct success of the genetic, biochemical, biophysical, and structural work was the identification of a product-dependent inhibitor. The chemical and biological advantages of product-dependent inhibition can be applied to other target enzymes, especially those having relatively large

active site pockets. The presence of a product or substrate in the active site(s) limits the size of the binding pocket, so that inhibitors can be more efficiently designed to fit the chemical property space required for the indication of interest.

4. GENERAL METHODS

Full methods are available in the Supporting Information. Bacterial strains and plasmids used in this study are listed in Table S1. MICs were determined by the broth dilution method. Genetic target identification was performed using materials and methods including spontaneous resistant mutant isolation, the mobile plasmid collection, genome sequencing, PCR, and DNA sequencing. LpxA-His6, biotinylated Avi-LpxA, and holo-ACP were overexpressed in *E. coli* and purified by chromatographic steps with appropriate enzymatic treatments. 3-OH-acyl-ACP was prepared by enzymatic acylation of holo-ACP and purification by chromatography. The in vitro LpxA biochemical reaction was performed by incubation of LpxA-His6 and the substrates for 15 min at room temperature, followed by SPE-MS detection of the generated LpxA product UDP-3-O-(*R*-3-hydroxymyristoyl)-GlcNAc using Agilent RapidFire 365 coupled to Sciex 5500 triple quadrupole MS. The LpxA SPR binding assay was performed using Biacore T200. Protein-observed NMR using isotope-enriched LpxA-His6 protein was performed as described previously.⁴³ The X-ray crystal structures of the LpxA/ligand complexes were obtained by crystal soaking and solved by molecular replacement. Compound 1 and 5-(4-methylpyridin-2-yl)-1*H*-pyrazole-3-carboxylic acid for compound 2 were prepared using literature procedures.^{55,56} Morpholine intermediates were purchased or prepared using two methods. Compound 2 and the analogues were prepared using three different methods including amide coupling of 5-(4-methylpyridin-2-yl)-1*H*-pyrazole-3-carboxylic acid and the corresponding morpholines. After LC-MS confirmation, compounds were extracted with ethyl acetate or dichloromethane and purified by reverse phase HPLC.

■ ASSOCIATED CONTENT

SI Supporting Information

The Supporting Information is available free of charge at <https://pubs.acs.org/doi/10.1021/jacs.9b13530>.

Full experimental methods and additional data and figures including IC₅₀ curves, chemical structures, SPR sensogram, dose response curve, 2D ¹H-¹³C HMQC spectra, and X-ray structures (PDF)

CIF files for crystallographic information (ZIP)

■ AUTHOR INFORMATION

Corresponding Author

Tsuyoshi Uehara – Novartis Institutes for BioMedical Research, Emeryville, California 94608, United States; orcid.org/0000-0001-6994-4286; Email: tsuyoshi.uehara@gmail.com

Authors

Wooseok Han – Novartis Institutes for BioMedical Research, Emeryville, California 94608, United States

Xiaolei Ma – Novartis Institutes for BioMedical Research, Emeryville, California 94608, United States; orcid.org/0000-0002-5307-827X

Carl J. Balibar – Novartis Institutes for BioMedical Research, Emeryville, California 94608, United States

Christopher M. Baxter Rath – Novartis Institutes for BioMedical Research, Emeryville, California 94608, United States

Bret Benton – Novartis Institutes for BioMedical Research, Emeryville, California 94608, United States

Alun Bermingham – Novartis Institutes for BioMedical Research, Emeryville, California 94608, United States

Fergal Casey – Novartis Institutes for BioMedical Research, Emeryville, California 94608, United States
Barbara Chie-Leon – Novartis Institutes for BioMedical Research, Emeryville, California 94608, United States
Min-Kyu Cho – Novartis Institutes for BioMedical Research, Cambridge, Massachusetts 02139, United States
Andreas O. Frank – Novartis Institutes for BioMedical Research, Emeryville, California 94608, United States
Alexandra Frommlet – Novartis Institutes for BioMedical Research, Emeryville, California 94608, United States
Chi-Min Ho – Novartis Institutes for BioMedical Research, Emeryville, California 94608, United States
Patrick S. Lee – Novartis Institutes for BioMedical Research, Emeryville, California 94608, United States
Min Li – Novartis Institutes for BioMedical Research, Emeryville, California 94608, United States
Andreas Lingel – Novartis Institutes for BioMedical Research, Emeryville, California 94608, United States; orcid.org/0000-0003-2909-4920
Sylvia Ma – Novartis Institutes for BioMedical Research, Emeryville, California 94608, United States
Hanne Merritt – Novartis Institutes for BioMedical Research, Emeryville, California 94608, United States
Elizabeth Ornelas – Novartis Institutes for BioMedical Research, Emeryville, California 94608, United States
Gianfranco De Pascale – Novartis Institutes for BioMedical Research, Emeryville, California 94608, United States
Ramadevi Prathapam – Novartis Institutes for BioMedical Research, Emeryville, California 94608, United States
Katherine R. Prosen – Novartis Institutes for BioMedical Research, Emeryville, California 94608, United States
Dita Rasper – Novartis Institutes for BioMedical Research, Emeryville, California 94608, United States
Alexey Ruzin – Novartis Institutes for BioMedical Research, Emeryville, California 94608, United States
William S. Sawyer – Novartis Institutes for BioMedical Research, Emeryville, California 94608, United States
Jacob Shaul – Novartis Institutes for BioMedical Research, Emeryville, California 94608, United States
Xiaoyu Shen – Novartis Institutes for BioMedical Research, Emeryville, California 94608, United States
Steven Shia – Novartis Institutes for BioMedical Research, Emeryville, California 94608, United States
Micah Steffek – Novartis Institutes for BioMedical Research, Emeryville, California 94608, United States
Sharadha Subramanian – Novartis Institutes for BioMedical Research, Emeryville, California 94608, United States
Jason Vo – Novartis Institutes for BioMedical Research, Emeryville, California 94608, United States
Feng Wang – Novartis Institutes for BioMedical Research, Emeryville, California 94608, United States
Charles Wartchow – Novartis Institutes for BioMedical Research, Emeryville, California 94608, United States

Complete contact information is available at:
<https://pubs.acs.org/10.1021/jacs.9b13530>

Author Contributions

• W.H. and X.M. contributed equally.

Funding

This work was funded by Novartis Institutes for BioMedical Research.

Notes

The authors declare the following competing financial interest(s): The authors are all current or former employees of the Novartis Institutes for Biomedical Research.

ACKNOWLEDGMENTS

We thank Catherine Jones for editorial support, and Angela DeLucia, Stacey Tiamfook, JoAnn Dzink-Fox, John Walker, Whitney Barnes, Javier de Vicente, Subramanian Karur, and Colin Skepper for experimental support. We also thank David Six, Charles Dean, Laura McDowell, Jennifer Leeds, Folkert Reck, Johanna Jansen, Isabel Zaror, Dirk Bussiere, Heinz Moser, Don Ganem, and past and present colleagues at Novartis Institutes for BioMedical Research in Emeryville, CA, for helpful discussion and support.

ABBREVIATIONS

LPS, lipopolysaccharide; ACP, acyl carrier protein; GlcNAc, *N*-acetylglucosamine; SPE-MS, solid-phase-extraction mass-spectrometry; MIC, minimal inhibitory concentration; SPR, surface plasmon resonance; HMQC, heteronuclear multiple quantum coherence

REFERENCES

- (1) Watkins, R. R.; Bonomo, R. A. Overview: Global and Local Impact of Antibiotic Resistance. *Infect Dis Clin North Am.* **2016**, *30* (2), 313–322.
- (2) Shlaes, D. M.; Bradford, P. A. Antibiotics—From There to Where? *Pathogens and Immunity* **2018**, *3* (1), 19–43.
- (3) Blair, J. M.; Webber, M. A.; Baylay, A. J.; Ogbolu, D. O.; Piddock, L. J. Molecular mechanisms of antibiotic resistance. *Nat. Rev. Microbiol.* **2015**, *13* (1), 42–51.
- (4) Tommasi, R.; Brown, D. G.; Walkup, G. K.; Manchester, J. I.; Miller, A. A. ESKAPEing the labyrinth of antibacterial discovery. *Nat. Rev. Drug Discovery* **2015**, *14* (8), 529–42.
- (5) Payne, D. J.; Gwynn, M. N.; Holmes, D. J.; Pompliano, D. L. Drugs for bad bugs: confronting the challenges of antibacterial discovery. *Nat. Rev. Drug Discovery* **2007**, *6* (1), 29–40.
- (6) Ho, H.; Miu, A.; Alexander, M. K.; Garcia, N. K.; Oh, A.; Zilberley, I.; Reichelt, M.; Austin, C. D.; Tam, C.; Shriver, S.; Hu, H.; Labadie, S. S.; Liang, J.; Wang, L.; Wang, J.; Lu, Y.; Purkey, H. E.; Quinn, J.; Franke, Y.; Clark, K.; Beresini, M. H.; Tan, M. W.; Sellers, B. D.; Maurer, T.; Koehler, M. F. T.; Weckler, A. T.; Kiefer, J. R.; Verma, V.; Xu, Y.; Nishiyama, M.; Payandeh, J.; Koth, C. M. Structural basis for dual-mode inhibition of the ABC transporter MsbA. *Nature* **2018**, *557* (7704), 196–201.
- (7) Zhang, G.; Baidin, V.; Pahil, K. S.; Moison, E.; Tomasek, D.; Ramadoss, N. S.; Chatterjee, A. K.; McNamara, C. W.; Young, T. S.; Schultz, P. G.; Meredith, T. C.; Kahne, D. Cell-based screen for discovering lipopolysaccharide biogenesis inhibitors. *Proc. Natl. Acad. Sci. U. S. A.* **2018**, *115* (26), 6834–6839.
- (8) Brown, D. G. Drug discovery strategies to outer membrane targets in Gram-negative pathogens. *Bioorg. Med. Chem.* **2016**, *24* (24), 6320–6331.
- (9) Richie, D. L.; Wang, L.; Chan, H.; De Pascale, G.; Six, D. A.; Wei, J. R.; Dean, C. R. A pathway-directed positive growth restoration assay to facilitate the discovery of lipid A and fatty acid biosynthesis inhibitors in *Acinetobacter baumannii*. *PLoS One* **2018**, *13* (3), No. e0193851.
- (10) Srinivas, N.; Jetter, P.; Ueberbacher, B. J.; Werneburg, M.; Zerbe, K.; Steinmann, J.; Van der Meijden, B.; Bernardini, F.; Lederer, A.; Dias, R. L.; Misson, P. E.; Henze, H.; Zumbrunn, J.; Gombert, F. O.; Obrecht, D.; Hunziker, P.; Schauer, S.; Ziegler, U.; Kach, A.; Eberl, L.; Riedel, K.; DeMarco, S. J.; Robinson, J. A. Peptidomimetic antibiotics target outer-membrane biogenesis in *Pseudomonas aeruginosa*. *Science* **2010**, *327* (5968), 1010–3.

- (11) Sherman, D. J.; Okuda, S.; Denny, W. A.; Kahne, D. Validation of inhibitors of an ABC transporter required to transport lipopolysaccharide to the cell surface in *Escherichia coli*. *Bioorg. Med. Chem.* **2013**, *21* (16), 4846–51.
- (12) Cohen, F.; Aggen, J. B.; Andrews, L. D.; Assar, Z.; Boggs, J.; Choi, T.; Dozzo, P.; Easterday, A. N.; Haglund, C. M.; Hildebrandt, D. J.; Holt, M. C.; Joly, K.; Jubb, A.; Kamal, Z.; Kane, T. R.; Konradi, A. W.; Krause, K. M.; Linsell, M. S.; Machajewski, T. D.; Miroschnikova, O.; Moser, H. E.; Nieto, V.; Phan, T.; Plato, C.; Serio, A. W.; Seroogy, J.; Shakhmin, A.; Stein, A. J.; Sun, A. D.; Sviridov, S.; Wang, Z.; Wlaschuk, K.; Yang, W.; Zhou, X.; Zhu, H.; Cirz, R. T. Optimization of LpxC Inhibitors for Antibacterial Activity and Cardiovascular Safety. *ChemMedChem* **2019**, *14*, 1560.
- (13) Tomaras, A. P.; McPherson, C. J.; Kuhn, M.; Carifa, A.; Mullins, L.; George, D.; Desbonnet, C.; Eidem, T. M.; Montgomery, J. I.; Brown, M. F.; Reilly, U.; Miller, A. A.; O'Donnell, J. P. LpxC inhibitors as new antibacterial agents and tools for studying regulation of lipid A biosynthesis in Gram-negative pathogens. *mBio* **2014**, *5* (5), No. e01551-14.
- (14) Erwin, A. L. Antibacterial Drug Discovery Targeting the Lipopolysaccharide Biosynthetic Enzyme LpxC. *Cold Spring Harbor Perspect. Med.* **2016**, *6* (7), a025304.
- (15) Lee, P. S.; Lapointe, G.; Madera, A. M.; Simmons, R. L.; Xu, W.; Yifru, A.; Tjandra, M.; Karur, S.; Rico, A.; Thompson, K.; Bojkovic, J.; Xie, L.; Uehara, K.; Liu, A.; Shu, W.; Bellamacina, C.; McKenney, D.; Morris, L.; Tonn, G. R.; Osborne, C.; Benton, B. M.; McDowell, L.; Fu, J.; Sweeney, Z. K. Application of Virtual Screening to the Identification of New LpxC Inhibitor Chemotypes, Oxazolidinone and Isoxazoline. *J. Med. Chem.* **2018**, *61*, 9360.
- (16) Kroeck, K. G.; Sacco, M. D.; Smith, E. W.; Zhang, X.; Shoun, D.; Akhtar, A.; Darch, S. E.; Cohen, F.; Andrews, L. D.; Knox, J. E.; Chen, Y. Discovery of dual-activity small-molecule ligands of *Pseudomonas aeruginosa* LpxA and LpxD using SPR and X-ray crystallography. *Sci. Rep.* **2019**, *9* (1), 15450.
- (17) Raetz, C. R.; Reynolds, C. M.; Trent, M. S.; Bishop, R. E. Lipid A modification systems in gram-negative bacteria. *Annu. Rev. Biochem.* **2007**, *76*, 295–329.
- (18) Onishi, H. R.; Pelak, B. A.; Gerckens, L. S.; Silver, L. L.; Kahan, F. M.; Chen, M. H.; Patchett, A. A.; Galloway, S. M.; Hyland, S. A.; Anderson, M. S.; Raetz, C. R. Antibacterial agents that inhibit lipid A biosynthesis. *Science* **1996**, *274* (5289), 980–2.
- (19) Lin, L.; Tan, B.; Pantapalankoor, P.; Ho, T.; Baquir, B.; Tomaras, A.; Montgomery, J. I.; Reilly, U.; Barbacci, E. G.; Hujer, K.; Bonomo, R. A.; Fernandez, L.; Hancock, R. E.; Adams, M. D.; French, S. W.; Buslon, V. S.; Spellberg, B. Inhibition of LpxC protects mice from resistant *Acinetobacter baumannii* by modulating inflammation and enhancing phagocytosis. *mBio* **2012**, *3* (5), 312-12.
- (20) Ma, X.; Prathapam, R.; Wartchow, C.; Chie-Leon, B.; Ho, C. M.; De Vicente, J.; Han, W.; Li, M.; Lu, Y.; Ramurthy, S.; Shia, S.; Steffek, M.; Uehara, T. Structural and biological basis of small molecule inhibition of *Escherichia coli* LpxD acyltransferase essential for lipopolysaccharide biosynthesis. *ACS Infect. Dis.* **2019**, in press. DOI: 10.1021/acscinfecdis.9b00127.
- (21) Moffatt, J. H.; Harper, M.; Harrison, P.; Hale, J. D.; Vinogradov, E.; Seemann, T.; Henry, R.; Crane, B.; St Michael, F.; Cox, A. D.; Adler, B.; Nation, R. L.; Li, J.; Boyce, J. D. Colistin resistance in *Acinetobacter baumannii* is mediated by complete loss of lipopolysaccharide production. *Antimicrob. Agents Chemother.* **2010**, *54* (12), 4971–7.
- (22) Powers, M. J.; Trent, M. S. Expanding the paradigm for the outer membrane: *Acinetobacter baumannii* in the absence of endotoxin. *Mol. Microbiol.* **2018**, *107* (1), 47–56.
- (23) Anderson, M. S.; Bull, H. G.; Galloway, S. M.; Kelly, T. M.; Mohan, S.; Radika, K.; Raetz, C. R. UDP-N-acetylglucosamine acyltransferase of *Escherichia coli*. The first step of endotoxin biosynthesis is thermodynamically unfavorable. *J. Biol. Chem.* **1993**, *268* (26), 19858–19865.
- (24) Wyckoff, T. J.; Raetz, C. R. The active site of *Escherichia coli* UDP-N-acetylglucosamine acyltransferase. Chemical modification and site-directed mutagenesis. *J. Biol. Chem.* **1999**, *274* (38), 27047–55.
- (25) Raetz, C. R.; Roderick, S. L. A left-handed parallel beta helix in the structure of UDP-N-acetylglucosamine acyltransferase. *Science* **1995**, *270* (5238), 997–1000.
- (26) Badger, J.; Chie-Leon, B.; Logan, C.; Sridhar, V.; Sankaran, B.; Zwart, P. H.; Nienaber, V. Structure determination of LpxA from the lipopolysaccharide-synthesis pathway of *Acinetobacter baumannii*. *Acta Crystallogr., Sect. F: Struct. Biol. Cryst. Commun.* **2012**, *68* (12), 1477–1481.
- (27) Smith, E. W.; Zhang, X.; Behzadi, C.; Andrews, L. D.; Cohen, F.; Chen, Y. Structures of *Pseudomonas aeruginosa* LpxA Reveal the Basis for Its Substrate Selectivity. *Biochemistry* **2015**, *54* (38), 5937–48.
- (28) Williams, A. H.; Raetz, C. R. Structural basis for the acyl chain selectivity and mechanism of UDP-N-acetylglucosamine acyltransferase. *Proc. Natl. Acad. Sci. U. S. A.* **2007**, *104* (34), 13543–50.
- (29) Jenkins, R. J.; Heslip, K. A.; Meagher, J. L.; Stuckey, J. A.; Dotson, G. D. Structural basis for the recognition of peptide RJPXD33 by acyltransferases in lipid A biosynthesis. *J. Biol. Chem.* **2014**, *289* (22), 15527–35.
- (30) Jenkins, R. J.; Dotson, G. D. Dual targeting antibacterial peptide inhibitor of early lipid A biosynthesis. *ACS Chem. Biol.* **2012**, *7* (7), 1170–7.
- (31) Williams, A. H.; Immormino, R. M.; Gewirth, D. T.; Raetz, C. R. Structure of UDP-N-acetylglucosamine acyltransferase with a bound antibacterial pentadecapeptide. *Proc. Natl. Acad. Sci. U. S. A.* **2006**, *103* (29), 10877–82.
- (32) Benson, R. E.; Gottlin, E. B.; Christensen, D. J.; Hamilton, P. T. Intracellular expression of Peptide fusions for demonstration of protein essentiality in bacteria. *Antimicrob. Agents Chemother.* **2003**, *47* (9), 2875–81.
- (33) Dangkulwanich, M.; Raetz, C. R. H.; Williams, A. H. Structure guided design of an antibacterial peptide that targets UDP-N-acetylglucosamine acyltransferase. *Sci. Rep.* **2019**, *9* (1), 3947.
- (34) Shapiro, A. B.; Ross, P. L.; Gao, N.; Livchak, S.; Kern, G.; Yang, W.; Andrews, B.; Thresher, J. A high-throughput-compatible fluorescence anisotropy-based assay for competitive inhibitors of *Escherichia coli* UDP-N-acetylglucosamine acyltransferase (LpxA). *J. Biomol. Screening* **2013**, *18* (3), 341–7.
- (35) Clements, J. M.; Coignard, F.; Johnson, I.; Chandler, S.; Palan, S.; Waller, A.; Wijkmans, J.; Hunter, M. G. Antibacterial activities and characterization of novel inhibitors of LpxC. *Antimicrob. Agents Chemother.* **2002**, *46* (6), 1793–9.
- (36) Mohan, S.; Kelly, T. M.; Eveland, S. S.; Raetz, C. R.; Anderson, M. S. An *Escherichia coli* gene (FabZ) encoding (3R)-hydroxymyristoyl acyl carrier protein dehydrase. Relation to fabA and suppression of mutations in lipid A biosynthesis. *J. Biol. Chem.* **1994**, *269* (52), 32896–32903.
- (37) Zeng, D.; Zhao, J.; Chung, H. S.; Guan, Z.; Raetz, C. R.; Zhou, P. Mutants resistant to LpxC inhibitors by rebalancing cellular homeostasis. *J. Biol. Chem.* **2013**, *288* (8), 5475–86.
- (38) Robins, L. I.; Williams, A. H.; Raetz, C. R. Structural basis for the sugar nucleotide and acyl-chain selectivity of *Leptospira interrogans* LpxA. *Biochemistry* **2009**, *48* (26), 6191–201.
- (39) Saka, K.; Tadenuma, M.; Nakade, S.; Tanaka, N.; Sugawara, H.; Nishikawa, K.; Ichiyoshi, N.; Kitagawa, M.; Mori, H.; Ogasawara, N.; Nishimura, A. A complete set of *Escherichia coli* open reading frames in mobile plasmids facilitating genetic studies. *DNA Res.* **2005**, *12* (1), 63–8.
- (40) Laursen, B. S.; Sorensen, H. P.; Mortensen, K. K.; Sperling-Petersen, H. U. Initiation of protein synthesis in bacteria. *Microbiol. Mol. Biol. Rev.* **2005**, *69* (1), 101–23.
- (41) Chapman-Smith, A.; Morris, T. W.; Wallace, J. C.; Cronan, J. E., Jr. Molecular recognition in a post-translational modification of exceptional specificity. Mutants of the biotinylated domain of acetyl-CoA carboxylase defective in recognition by biotin protein ligase. *J. Biol. Chem.* **1999**, *274* (3), 1449–57.

(42) Baba, T.; Ara, T.; Hasegawa, M.; Takai, Y.; Okumura, Y.; Baba, M.; Datsenko, K. A.; Tomita, M.; Wanner, B. L.; Mori, H. Construction of *Escherichia coli* K-12 in-frame, single-gene knockout mutants: the Keio collection. *Mol. Syst. Biol.* **2006**, *2*, 2006-0008.

(43) Proudfoot, A.; Frank, A. O.; Frommlet, A.; Lingel, A. Selective Methyl Labeling of Proteins: Enabling Structural and Mechanistic Studies As Well As Drug Discovery Applications by Solution-State NMR. *Methods Enzymol.* **2019**, *614*, 1–36.

(44) Proudfoot, A.; Frank, A. O.; Ruggiu, F.; Mamo, M.; Lingel, A. Facilitating unambiguous NMR assignments and enabling higher probe density through selective labeling of all methyl containing amino acids. *J. Biomol. NMR* **2016**, *65* (1), 15–27.

(45) Chen, V. B.; Arendall, W. B., 3rd; Headd, J. J.; Keedy, D. A.; Immormino, R. M.; Kapral, G. J.; Murray, L. W.; Richardson, J. S.; Richardson, D. C. MolProbity: all-atom structure validation for macromolecular crystallography. *Acta Crystallogr., Sect. D: Biol. Crystallogr.* **2010**, *66* (1), 12–21.

(46) O'Shea, R.; Moser, H. E. Physicochemical properties of antibacterial compounds: implications for drug discovery. *J. Med. Chem.* **2008**, *51* (10), 2871–8.

(47) Brown, D. G.; May-Dracka, T. L.; Gagnon, M. M.; Tommasi, R. Trends and exceptions of physical properties on antibacterial activity for Gram-positive and Gram-negative pathogens. *J. Med. Chem.* **2014**, *57* (23), 10144–61.

(48) Heath, R. J.; Rubin, J. R.; Holland, D. R.; Zhang, E.; Snow, M. E.; Rock, C. O. Mechanism of triclosan inhibition of bacterial fatty acid synthesis. *J. Biol. Chem.* **1999**, *274* (16), 11110–4.

(49) Kalinin, D. V.; Holl, R. LpxC inhibitors: a patent review (2010–2016). *Expert Opin. Ther. Pat.* **2017**, *27* (11), 1227–1250.

(50) Sivaraman, S.; Zwahlen, J.; Bell, A. F.; Hedstrom, L.; Tonge, P. J. Structure-activity studies of the inhibition of FabI, the enoyl reductase from *Escherichia coli*, by triclosan: kinetic analysis of mutant FabIs. *Biochemistry* **2003**, *42* (15), 4406–13.

(51) Richter, M. F.; Drown, B. S.; Riley, A. P.; Garcia, A.; Shirai, T.; Svec, R. L.; Hergenrother, P. J. Predictive compound accumulation rules yield a broad-spectrum antibiotic. *Nature* **2017**, *545* (7654), 299–304.

(52) Six, D. A.; Krucker, T.; Leeds, J. A. Advances and challenges in bacterial compound accumulation assays for drug discovery. *Curr. Opin. Chem. Biol.* **2018**, *44*, 9–15.

(53) Iyer, R.; Ye, Z.; Ferrari, A.; Duncan, L.; Tanudra, M. A.; Tsao, H.; Wang, T.; Gao, H.; Brummel, C. L.; Erwin, A. L. Evaluating LC-MS/MS To Measure Accumulation of Compounds within Bacteria. *ACS Infect. Dis.* **2018**, *4* (9), 1336–1345.

(54) Wyckoff, T. J.; Lin, S.; Cotter, R. J.; Dotson, G. D.; Raetz, C. R. Hydrocarbon rulers in UDP-N-acetylglucosamine acyltransferases. *J. Biol. Chem.* **1998**, *273* (49), 32369–72.

(55) Alanazi, A. M.; El-Azab, A. S.; Al-Swaidan, I. A.; Maarouf, A. R.; El-Bendary, E. R.; Abu El-Enin, M. A.; Abdel-Aziz, A. A.-M. *Med. Chem. Res.* **2013**, *22* (12), 6129–6142.

(56) Short, K. M.; Pham, S. M.; Williams, D. C.; Datta, S. Multisubstituted aromatic compounds as inhibitors of thrombin. US Patent 9533967 B2, 2017.